ELSEVIER

Nuclear Physics B (Proc. Suppl.) 122 (2003) 317–320

NUCLEAR PHYSICS B
PROCEEDINGS
SUPPLEMENTS

www.elsevier.com/locate/npe

Determination of primary energy and mass in the PeV region by Bayesian unfolding techniques

M. Roth[a*], T. Antoni[b], W.D. Apel[a], F. Badea[b†], K. Bekk[a], A. Bercuci[a†], H. Blümer[a,b], H. Bozdog[a], I.M. Brancus[c], C. Büttner[a], A. Chilingarian[d], K. Daumiller[b], P. Doll[a], J. Engler[a], F. Feßler[a], H.J. Gils[a], R. Glasstetter[b], R. Haeusler[b], A. Haungs[a], D. Heck[a], J.R. Hörandel[b], A. Iwan[b‡], K.-H. Kampert[b,a], H.O. Klages[a], G. Maier[a], H.J. Mathes[a], H.J. Mayer[a], J. Milke[a], M. Müller[a], R. Obenland[a], J. Oehlschläger[a], S. Ostapchenko[b§], M. Petcu[c], H. Rebel[a], M. Risse[a], G. Schatz[a], H. Schieler[a], J. Scholz[a], T. Thouw[a], H. Ulrich[b], J.H. Weber[b], A. Weindl[a], J. Wentz[a], J. Wochele[a], J. Zabierowski[e]

[a]Institut für Kernphysik, Forschungszentrum Karlsruhe, 76021 Karlsruhe, Germany
[b]Institut für Experimentelle Kernphysik, Universität Karlsruhe, 76021 Karlsruhe, Germany
[c]National Institute of Physics and Nuclear Engineering, 7690 Bucharest, Romania
[d]Cosmic Ray Division, Yerevan Physics Institute, Yerevan 36, Armenia
[e]Soltan Institute for Nuclear Studies, 90950 Lodz, Poland

The field detector array of the KASCADE experiment measures the electron and muon component of extensive air showers in the knee region with high precision. A baysian unfolding procedure is presented in which the two-dimensional shower size distribution (N_e, N_μ^{tr}) is examined. On the arbitrary assumption that the chemical composition consists of five primary mass groups (hydrogen, helium, carbon, silicon and iron) the size distribution is deconvoluted to reconstruct the energy spectra of these mass groups in the energy range between 10^{15} eV and 10^{17} eV. The energy spectra of the lighter element groups result in a knee-like bending with a steepening above the knee. The topology of the individual knee positions suggest a rigidity dependence.

1. Introduction

The knowledge of the energy spectra of different components of primary cosmic rays in the knee region is of vital importance for testing alternative hypotheses of the cosmic ray (CR) origin and acceleration. The presented analysis of EAS benefits from the simultaneous measurement of different observables for each individual event by the KASCADE experiment [1]. Appropriate unfolding procedures taking correlations into account make it possible to deconvolute such multidimensional size distributions and result in energy spectra for various primary mass groups.

2. Simulation and Reconstruction

The analysis is based on a large set of CORSIKA simulation patterns [2] including a full simulation of the detector response. The simulations have been performed using the interaction model QGSJET (vers. of 1998) [3]. For low-energy interactions the GHEISHA code [4] is invoked. Samples of about 130,000 proton, helium, carbon, silicon, and iron-induced showers have been simulated. The centres of the showers are spread uniformly over the area of the detector array. The energy distribution follows a power law with a spectral index of -2 in the energy range 10^{14} eV to 10^{17} eV and the zenith angles are distributed in the range $[0°, 42°]$. The method described below is applied on size spectra for 3 individual angular intervals and the resulting spectra are combined to increase the statistics.

*corresponding author, e-mail: markus.roth@ik.fzk.de
†on leave of absence from National Institute of Physics and Nuclear Engineering, Bucharest, Romania
‡on leave of absence from University of Lodz, Poland
§on leave of absence from Moscow State University Moscow, Russia

doi:10.1016/S0920-5632(03)02036-X

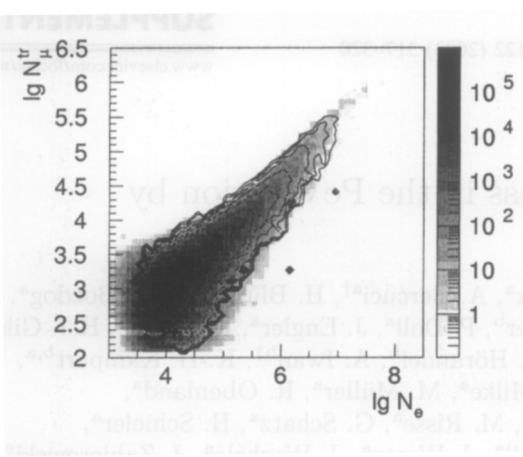

Figure 1. The measured size spectrum (grey scale) is compared with the reconstructed distribution (contour); $\theta \in [0°, 18°]$.

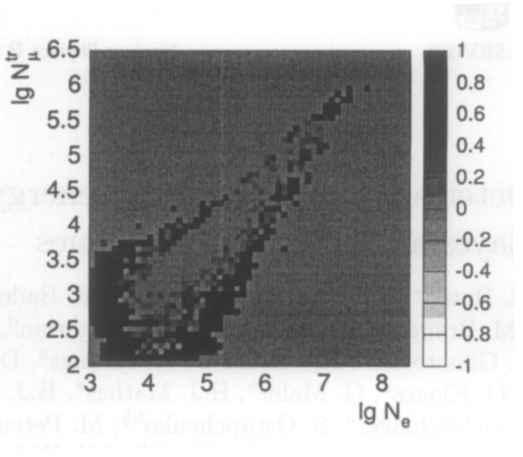

Figure 2. The difference $(N_{exp} - N_{MC})/N_{exp}$ between experimental and simulated data is displayed; $\theta \in [0°, 18°]$.

3. Bayesian Unfolding

In general the process of measuring distributions of physical observables $g(N_e, N_\mu^{tr})$ is often disturbed by inherent limitations which lead to the nontrivial problem of inferring true distributions from measured ones. Confining conditions like limited acceptance or efficiency of the detector arrangement, finite resolution, strong intrinsic fluctuations and parameter transformations have to be taken into account to solve the inverse problem. Suitable methods to infer physical quantities are unfolding algorithms based on *Fredholm integral equations of* 1^{st} *kind*

$$g_i(N_e, N_\mu^{tr}) = \int_0^\infty t_i(N_e, N_\mu^{tr}|E) p_i(E) dE \qquad (1)$$

where the transfer function $t_i(N_e, N_\mu^{tr}|E)$ ($i \in$ {p, He, C, Si, Fe}) has to cover all the above mentioned limiting effects and is realized by means of detailed Monte Carlo (MC) simulations. Various mathematical methods and variants of unfolding procedures [5,6] exist to determine the energy distribution $p_i(E)$ for the different masses i. To crosscheck systematic uncertainties due to the method applied, KASCADE data are analysed with conceptually different algorithms: a Bayesian approach presented in this paper, neural network and Bayesian classifier algorithms [7] and a Gold unfolding method described in Ref. [8]. The used Bayesian unfolding method [5] is a powerful algorithm which allows to analyse multidimensional data sets (N_e, N_μ^{tr}) (see Fig. 1) and is capable to propagate errors of both Monte Carlo statistics and measured data [5]. For sake of simplicity only one primary mass is considered in the following, but the method can easily be extended to cope with more than just one mass group. Arranging measured and simulated data in histograms one is dealing with sums of matrices but no more with integrals from Eq. 1. Evidently the applied unfolding method is based on Bayes' Theorem

$$P(E_i|N_e, N_\mu^{tr}) = \frac{P(N_e, N_\mu^{tr}|E_i) \cdot P_0(E_i)}{\sum_{l=1}^{n_E} P(N_e, N_\mu^{tr}|E_l) \cdot P_0(E_l)} \qquad (2)$$

If a single event (N_e, N_μ^{tr}) is observed, the probability that it is caused by the i-th unknown energy E_i is proportional to the probability of the cause E_i times the probability of the cause to produce the observation (N_e, N_μ^{tr}) (normalised to unity). Thus the general idea is to connect initial and measured distributions by assuming *a priori* knowledge, i.e. $P_0(E_i)$. If $n(N_e, N_\mu^{tr})$ events are observed, the expected number of events assigned to each of the causes is

$$\hat{n}(E_i) = n(N_e, N_\mu^{tr}) \cdot P(E_i|N_e, N_\mu^{tr}) \qquad (3)$$

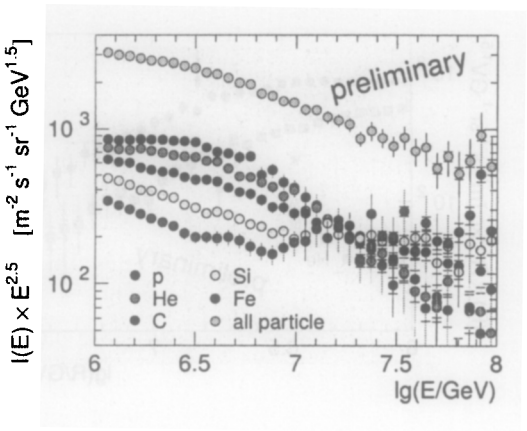

Figure 3. Result of the Bayesian unfolding procedure. Ticked Error bars correspond to the error of the reconstructed number of events. The grey coloured error bars reflect the propagated error due to finite MC and measurement statistics.

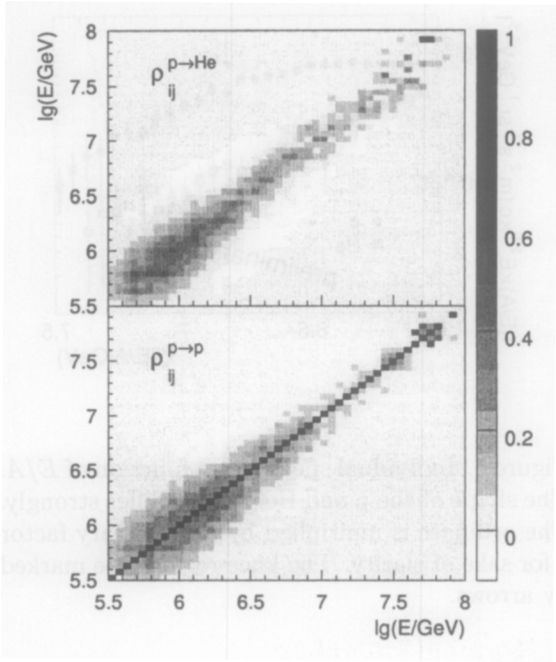

Figure 4. Correlation matrices of the Bayesian Unfolding procedure. The upper panel displays the correlation between proton energy bins (abscissa) and Helium energy bins (ordinate). The lower graph displays the correlation of different energy bins of the reconstructed proton spectrum.

As the outcome of measurements one has several possible effects $n(N_{e,j}, N^{tr}_{\mu,j})$ ($j \in \{1,\ldots,n_N\}$ is the corresponding bin) for a given cause E_i. For each of them the Bayes formula Eq. 2 holds and $P(E_i|N_{e,j}, N^{tr}_{\mu,j})$ can be evaluated. Finally the expected number of events to be assigned to each of the causes and only due to the observed events can be calculated applying Eq. 3 to each of the effects

$$\hat{n}(E_i)|_{obs} = \sum_{j=1}^{n_N} n(N_{e,j}, N^{tr}_{\mu,j}) \cdot P(E_i|N_{ej}, N^{tr}_{\mu j}) \quad (4)$$

The final estimate $\hat{n}(E_i)|_{obs}$ of the initial (physical) energy distribution $P_0(E_i)$ is determined in an iterative procedure and Eq. 4 might be interpreted as the discrete inversion of Eq. 1.

4. Results and Conclusion

After applying the algorithm the reconstructed size distribution $\hat{g}(N_e, N^{tr}_{\mu})$ can be compared with experimental data as shown in Fig. 1. The difference plot in Fig. 2 reveals several difficulties. First of all the lack of MC data at the threshold prevents to extract the energy spectrum at energies less than 10^{15} eV. In addition, the limited MC statistics does not allow to describe the regions of small statistics. Especially a band along the *proton region* occurs (lower bound of the contour) reflecting the fact, that protons have large fluctuations, which are not well reproduced by the limited MC proton statistics. The resulting energy spectra are shown in Fig. 3. The knee in the total energy spectrum at about 5-6 PeV is caused mostly by the steepening of the spectra of the light components. The all particle spectrum agrees not only with the results of the aforementioned neural network analysis [7] but also with the outcome of a Gold unfolding method [8] corroborating the results described in this paper. The correlation matrix $\rho_{ij} = \sigma_{ij}/\sigma_i \cdot \sigma_j$ displayed in Fig. 4 shows clearly crosstalk between individual energy bins not only for each single mass group

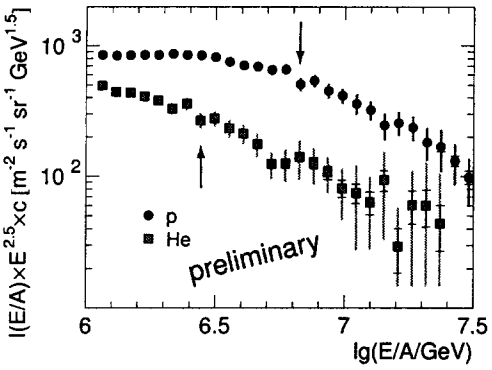

Figure 5. Individual spectra as a function of E/A. The shape of the p and He spectra differ strongly. The ordinate is multiplied by an arbitrary factor c for sake of clarity. The knee regions are marked by arrows.

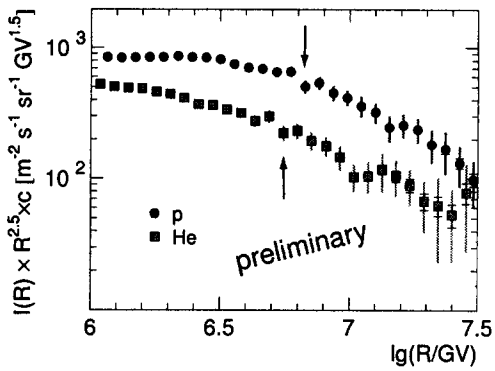

Figure 6. Individual spectra as a function of the rigidity R. The shape of the p and He spectra are nearly congruent and the knee positions are nearly at the same position $\lg(R/GV) = 6.75$.

(lower panel), but also between energy bins of different primaries (e.g. $\rho_{ij}^{p \to He}$ upper panel). The error bars in Figs. 3, 5 and 6 show uncertainties, which are calculated by error propagation using σ_{ij}.

The position of the steepening of the spectrum is shifted to higher energies for heavier components. To investigate the energy dependency the statistical most significant spectra of p and He are shown as a function of E/A in Fig. 5 and as a function of the rigidity $R = E/Z$ in Fig. 6. As a preliminary result a rigidity dependent knee energy seems to be favoured by comparing the shape and the knee energy of the individual spectra. But by far more MC data have to be simulated to reduce the large systematic uncertainties and to make any quantitative conclusion feasible. In addition systematic studies with different other interaction models are necessary to exclude distortions from a specific model assumption guiding to a biased result.

Acknowledgement *The KASCADE experiment is supported by collaborative WTZ projects in the frame of the scientific-technical cooperation between Germany and Romania (RUM 97/014), Poland (POL 99/005) and Armenia (ARM 98/002). The Polish group (Soltan Institute and University of Lodz) acknowledges the support by the Polish State Committee for Scientific Research (grant No. 5 P03B 133 20). The author M. R. gratefully acknowledges the supported grant by the Alexander von Humboldt foundation.*

REFERENCES

1. H.O. Klages et al., Nucl. Phys. B, Proc. Suppl., 52B (1997) 92.
2. D. Heck et al., FZKA 6019, Forschungszentrum Karlsruhe, 1998.
3. N.N. Kalmykov and S.S. Ostapchenko, Yad. Fiz. 56 (1993) 105.
4. H. Fesefeldt, PITHA-85/02, RWTH Aachen, 1985.
5. G. D'Agostini, Nucl. Instr. and Meth. in Phys. Res., A362, 487,1995.
6. R. Gold, ANL-6984, Argonne National Laboratory Report, 1964.
7. T. Antoni et al., KASCADE Collaboration, Astrop. Phys. 16 (2002) 245; M. Roth et al., KASCADE Collaboration, 27^{th} ICRC, Hamburg (2001) 88.
8. H. Ulrich et al., KASCADE Collaboration, 27^{th} ICRC, Hamburg (2001) 97; H. Ulrich et al., in these proceedings.